

# Stable branches of a solution for a fermion on domain wall

V. A. Gani<sup>1,2</sup>, V. G. Ksenzov<sup>2</sup>, A. E. Kudryavtsev<sup>2</sup>

<sup>1</sup>*Department of Mathematics, National Research Nuclear University MEPhI,*

*Moscow 115409, Russia.*

<sup>2</sup>*State Scientific Center Institute for Theoretical and Experimental Physics,*

*Moscow 117218, Russia.*

## Abstract

We discuss the case when a fermion occupies an excited non-zero frequency level in the field of domain wall. We demonstrate that a solution exists for the coupling constant in the limited interval  $1 < g < g_{max} \approx 1.65$ . We show that indeed there are different branches of stable solution for  $g$  in this interval. The first one corresponds to a fermion located on the domain wall ( $1 < g < \sqrt[4]{2\pi}$ ). The second branch, which belongs to the interval  $\sqrt[4]{2\pi} \leq g \leq g_{max}$ , describes a polarized fermion off the domain wall. The third branch with  $1 < g < g_{max}$  describes an excited antifermion in the field of the domain wall.

## 1 Introduction

In our previous paper [1] we studied the problem "domain wall + excited fermion". Initially the problem of the spectrum of a fermion coupled to the field of a static kink was discussed in Refs. [2, 3, 4, 5, 6]. These papers were devoted mainly to a zero-frequency fermion bound by the domain wall.

Fermionic bound states in the field of external kink were studied in Ref. [7] for the case of the  $\lambda\phi^4$ -model and in Ref. [8] for the case of the sine-Gordon model. However, the authors of these publications have considered kink as given external field. As we shall demonstrate in this our work, the presence of the fermion changes drastically the kink profile. So the excitation spectrum for the problem "fermion coupled to kink" looks quite different from that calculated in the external field approximation.

We studied the system of the interacting scalar ( $\phi$ ) and fermion ( $\Psi$ ) fields in two-dimensional space-time  $(1+1)$ . In terms of dimensionless fields, coupling constant  $g$  and space-time variables  $(x, t)$ , the Lagrangian density was taken in the form

$$\mathcal{L} = \frac{1}{2} (\partial_\mu \phi)^2 - \frac{1}{2} (\phi^2 - 1)^2 + \bar{\Psi} i \hat{\partial} \Psi - g \bar{\Psi} \Psi \phi. \quad (1.1)$$

The equation of motion for scalar field  $\phi(x, t)$  in the presence of a fermionic field  $\Psi$  reads:

$$\partial_\mu \partial^\mu \phi - 2\phi + 2\phi^3 = -g \bar{\Psi} \Psi, \quad (1.2)$$

where  $\bar{\Psi} = \Psi^\dagger \beta$ ,  $\beta$  is the Pauli matrix, see (1.5).

If the coupling of the scalar field to fermions is switched off,  $g = 0$ , the equation of motion (1.2) has a static solution called "kink",

$$\phi_K(x) = \tanh x. \quad (1.3)$$

In three space dimensions this solution corresponds to a domain wall that separates two space regions with different vacua  $\phi_\pm = \pm 1$ , see, e.g. [9, 10] for more details.

Let us discuss the fermionic sector of the theory. After the substitution  $\Psi(x, t) = e^{-i\varepsilon t} \psi_\varepsilon(x)$  the Dirac equation for the massless case reads:

$$\left( \varepsilon + i\alpha_x \frac{\partial}{\partial x} - g\beta\phi(x) \right) \psi_\varepsilon(x) = 0, \quad (1.4)$$

where  $\alpha_x$  and  $\beta$  are the Pauli matrices,

$$\alpha_x = \begin{pmatrix} 0 & -i \\ i & 0 \end{pmatrix}, \quad \beta = \begin{pmatrix} 0 & 1 \\ 1 & 0 \end{pmatrix}. \quad (1.5)$$

In equation (1.4),

$$\psi_\varepsilon(x) = \begin{pmatrix} u_\varepsilon(x) \\ v_\varepsilon(x) \end{pmatrix}$$

is the two-component spinor wave function. In terms of functions  $u_\varepsilon(x)$  and  $v_\varepsilon(x)$ , Eq. (1.4) takes the form

$$\begin{cases} \frac{du_\varepsilon}{dx} + g\phi(x)u_\varepsilon = \varepsilon v_\varepsilon, \\ -\frac{dv_\varepsilon}{dx} + g\phi(x)v_\varepsilon = \varepsilon u_\varepsilon. \end{cases} \quad (1.6)$$

Substituting  $\phi(x) = \phi_K(x) = \tanh x$  we finally get:

$$\begin{cases} -\frac{d^2u_\varepsilon}{dx^2} - \frac{g(g+1)}{\cosh^2 x}u_\varepsilon = (\varepsilon^2 - g^2)u_\varepsilon, \\ -\frac{d^2v_\varepsilon}{dx^2} - \frac{g(g-1)}{\cosh^2 x}v_\varepsilon = (\varepsilon^2 - g^2)v_\varepsilon. \end{cases} \quad (1.7)$$

This system describes the spectrum and eigenfunctions of the fermion in the external scalar field  $\phi_K(x) = \tanh x$ . Solutions of Eq. (1.7) with  $\varepsilon^2 \geq g^2$  belong to the continuum and those with  $\varepsilon^2 < g^2$  to the bound states. The best known discrete mode is the so-called zero-mode solution (it is time-independent,  $\varepsilon = 0$ ):

$$\Psi_{\varepsilon=0}(x) = \sqrt{\frac{\Gamma(g+1/2)}{\sqrt{\pi}\Gamma(g)}} \begin{pmatrix} \frac{1}{\cosh^g x} \\ 0 \end{pmatrix}. \quad (1.8)$$

For zero-mode solution (1.8) the r.h.s. of Eq. (1.2)  $\bar{\Psi}\Psi = 2uv \equiv 0$ , so we conclude that the solution of the full problem in the form " $\phi_K(x)$  + zero-mode bound fermion (1.8)" is self-consistent.

However, if the fermion occupies a level with  $\varepsilon \neq 0$ , the r.h.s. of Eq. (1.2) is different from zero. Hence the kink's profile has to be modified to fulfil Eq. (1.2). In our previous paper [1] we found one example of analytic solution for the excited fermion on a distorted domain wall, which indeed is self-consistent.

The plan of this our paper is the following. In Section 2 we study solutions for the first excited mode. We develop a simple variational procedure that allows to get a reasonable approximation to the solution for coupling constant  $g$  in the interval  $1 < g \leq g_{max} \approx 1.65$ . For  $g_1 = 2\sqrt{2(2 - \sqrt{3})} \approx 1.46$  the approximation coincides with the exact solution, found earlier in [1]. In Section 3 we present detailed analysis for the obtained solutions. In particular, we demonstrate that, depending on the coupling constant, we get two solution branches for the excited fermion on domain wall. For the coupling constant in the interval  $1 < g < \sqrt[4]{2\pi}$  the excited fermion is practically localized on a distorted domain wall. In the interval of couplings  $\sqrt[4]{2\pi} \leq g \leq g_{max}$  the initial profile of the domain wall, Eq. (1.3), is almost restored. We also found solution for an excited antifermion (i.e. solution with  $\varepsilon < 0$ ) on the domain wall. This solution looks like a smooth function without cuts or jumps for any coupling constants  $g$  in the interval  $g \in (1; g_{max}]$ .

At the same time for interval of the coupling  $\sqrt[4]{2} < g < g_{max}$  the two components of fermionic wave function behave very differently with respect to localization. Namely, the upper component  $u_\varepsilon(x)$  of the spinor  $\psi_\varepsilon(x)$  is located outside the domain wall, while the lower component  $v_\varepsilon(x)$  of the fermion wave function sits on the domain wall. So in this interval of  $g$  the domain wall separates in space the localizations of the upper and the lower components of the spinor.

A general discussion and the summary of the results are presented in Section 4.

## 2 Self-consistent solutions for fermion in the field of kink

Let us look for a solution of the Dirac equation for the fermion in the field of a distorted kink  $\tilde{\phi}_K = \tanh \alpha x$ , where  $\alpha$  is unknown real parameter to be determined from a self-consistency condition, as it will be discussed below. Introducing a new variable  $y = \alpha x$  and a new parameter  $s = g/\alpha$ , we get a system of equations for the fermionic wave

function, which formally coincides with that given by Eq. (1.7):

$$\begin{cases} -\frac{d^2 u_{\varepsilon'}}{dy^2} - \frac{s(s+1)}{\cosh^2 y} u_{\varepsilon'} = (\varepsilon'^2 - s^2) u_{\varepsilon'}, \\ -\frac{d^2 v_{\varepsilon'}}{dy^2} - \frac{s(s-1)}{\cosh^2 y} v_{\varepsilon'} = (\varepsilon'^2 - s^2) v_{\varepsilon'}. \end{cases} \quad (2.1)$$

Here  $\varepsilon' = \varepsilon/\alpha$ . The wave function of the fermion for the first excited state in the field of the distorted kink  $\tilde{\phi}_K$  reads ( $1 < s < +\infty$ ):

$$\psi_{\varepsilon'}(x) = \begin{pmatrix} u_{\varepsilon'}(x) \\ v_{\varepsilon'}(x) \end{pmatrix} = \sqrt{\frac{\alpha \Gamma(s-1/2)}{2\sqrt{\pi} \Gamma(s-1)}} \begin{pmatrix} \sqrt{2s-1} \frac{\tanh \alpha x}{\cosh^{s-1} \alpha x} \\ \frac{1}{\cosh^{s-1} \alpha x} \end{pmatrix}, \quad (2.2)$$

Substituting wave function (2.2) and  $\phi_K(x) = \tanh \alpha x$  into equation (1.2), we get that for  $s = 2$  and  $\varepsilon' = \sqrt{3}$  the self-consistency equation (1.2) is fulfilled if only the slope  $\alpha$  satisfies the condition [1]:

$$2\alpha^2 - 2 = -\sqrt{3}\alpha^2 \implies \alpha^2 = 2(2 - \sqrt{3}). \quad (2.3)$$

So for the special case of  $s = 2$  we obtain an analytic self-consistent solution for the problem of an excited fermion on the domain wall<sup>1</sup>. This solution corresponds to the value of coupling constant

$$g = g_1 = 2\sqrt{2(2 - \sqrt{3})} \approx 1.46.$$

For arbitrary  $s \in (1; +\infty)$ ,  $s \neq 2$  there is no analytic solution of equation (1.2) in the form  $\phi(x) = \tanh \alpha x$ . Substituting (2.2) into (1.2) we obtain the following constraint:

$$2\alpha^2 - 2 = -\frac{\alpha^2 s \Gamma(s-1/2) \sqrt{2s-1}}{\sqrt{\pi} \Gamma(s-1)} \frac{1}{\cosh^{2s-4} \alpha x}. \quad (2.4)$$

This constraint becomes an algebraic equation for  $\alpha$  in the limit  $s \rightarrow 1$ , (and  $g = 1$ ) with  $\alpha = 1$ , and also for  $s = 2$  (and  $g = g_1$ ) with  $\alpha = \alpha(2) = \sqrt{2(2 - \sqrt{3})}$ . The latter case corresponds to the exact solution discussed above, see Eq. (2.3).

---

<sup>1</sup>For  $s = 2$  and  $\varepsilon' = -\sqrt{3}$  we get analytic solution for an antifermion on the domain wall. Its wave function is also given by Eq. (2.2).

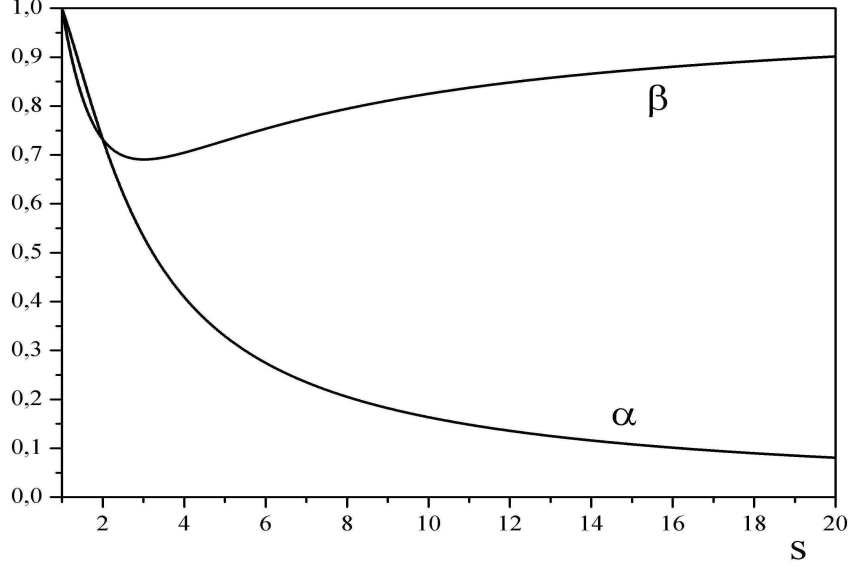


Figure 1: slopes  $\alpha(s)$  and  $\beta(s)$ .

However, Eq. (2.4) may be used to determine the slope  $\alpha(s)$  at  $x = 0$  for the fermionic wave function at arbitrary  $s \in (1; +\infty)$ . The function  $\alpha(s)$  is shown in Fig. 1. Note that for large  $s \gg 1$

$$\alpha(s) \approx \frac{\sqrt[4]{2\pi}}{s}$$

and  $\lim_{s \rightarrow +\infty} \alpha(s) = 0$ .

Inserting fermionic wave function (2.2) with the so obtained  $\alpha(s)$  into the r.h.s. of Eq. (1.2), we get the following equation for the scalar field  $\phi(x)$ :

$$\frac{d^2\phi}{dx^2} + 2\phi - 2\phi^3 = \frac{\alpha^2(s) s \sqrt{2s-1} \Gamma(s-1/2)}{2\sqrt{\pi} \Gamma(s-1)} \frac{\tanh(\alpha(s) x)}{\cosh^{2s-2}(\alpha(s) x)}. \quad (2.5)$$

This equation has no solutions for boundary conditions  $\phi_s(0) = 0$ ,  $\frac{d\phi_s(0)}{dx} = \alpha(s)$ ,  $\phi \rightarrow 1$  with  $x \rightarrow +\infty$  at arbitrary  $s \in (1; +\infty)$ . The only exceptional cases are those with  $s = 1$  and  $s = 2$ , for which we found exact solutions discussed above. However, one may try to solve the equation of motion (2.5) with modified boundary conditions for the field  $\phi_s(x, 0)$ :

$$\phi_s(0) = 0, \quad \frac{d\phi_s(0)}{dx} = \beta(s), \quad \lim_{x \rightarrow +\infty} \phi_s(x) = 1. \quad (2.6)$$

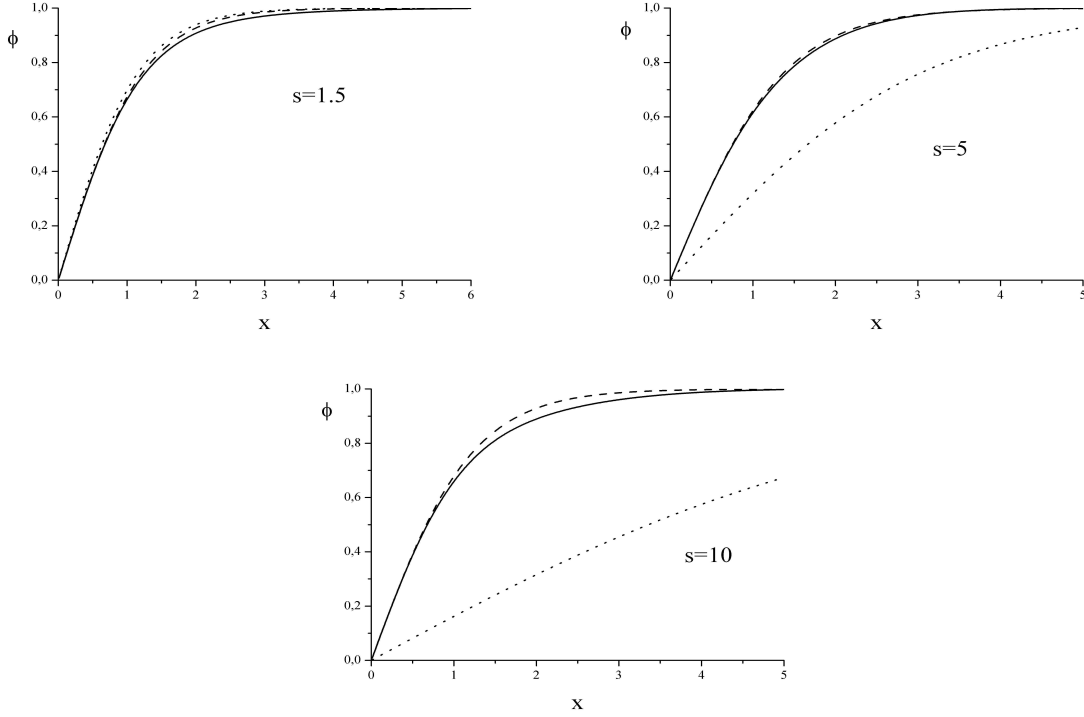


Figure 2: profiles of scalar field  $\phi_s(x)$  at different values of parameter  $s$ . Solid line – numerical solution of eq. (2.5); dashed line – approximation of the exact solution by  $\phi_s(x) = \tanh(\beta(s)x)$ . Dotted line – the function  $\phi_s^{in}(x) = \tanh(\alpha(s)x)$ .

We solved Eq. (2.5) with boundary conditions (2.6) numerically, using the shooting method for the whole interval of parameter  $s \in (1; +\infty)$ . The resulting function  $\beta(s)$  is shown in Fig. 1. Note that  $\beta(s) = \alpha(s)$  at two points  $s = 1$  and  $s = 2$ , for which our procedure reproduces exact solutions. In the region of small  $s \in (1; 2)$  functions  $\beta(s)$  and  $\alpha(s)$  do not differ drastically. On the other hand,  $\lim_{s \rightarrow +\infty} \beta(s) = 1$ , what means that our solution for scalar field approaches undistorted kink in the limit of large  $s$ .

Numerical solutions for the scalar field  $\phi_s(x)$  at different values of parameter  $s$  are given in Fig. 2, where we also show the profile of the function  $\tilde{\phi}_s(x) = \tanh(\beta(s)x)$ . This figure illustrates that for all  $s \in (1; +\infty)$  the exact numerical solution is very close to  $\tanh(\beta(s)x)$ . So one can say that with high accuracy the field configuration  $\phi_s(x)$  is a distorted kink with the slope  $\beta(s)$  at the origin.

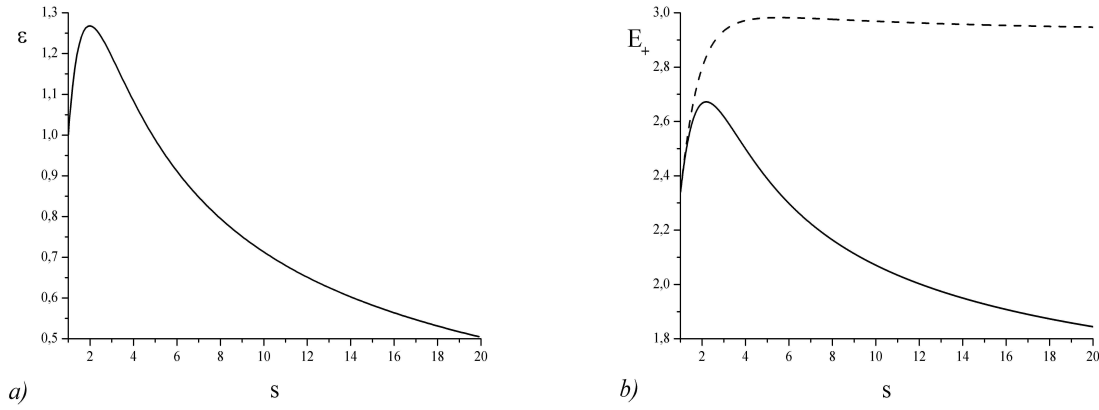


Figure 3: a) the energy of the fermion field  $\varepsilon(s)$ ; b) total energy of the system "kink + excited bound fermion"  $E_+(s)$  (solid line), the boundary line of the region "domain wall + fermion in continuum" (dashed line).

In terms of fields  $\{\phi_s(x); \Psi_s(x)\}$  the procedure we used here is indeed a variational-type one. This approximate procedure reproduces exact solutions for  $s = 1, 2$  and gives reasonable results in the whole range of parameter  $s$ .

### 3 Stable branches of solution for a fermion coupled to domain wall

The energy of a massless fermion in the field of the distorted kink  $\phi_K(\alpha(s)x)$  is  $\varepsilon(s) = \sqrt{2s-1} \alpha(s)$  and  $-\varepsilon(s)$  for massless antifermion. The function  $\varepsilon(s)$  is shown in Fig. 3a. Note that for large  $s \gg 1$   $\varepsilon(s)$  goes to zero,  $\varepsilon(s) \approx \frac{\sqrt[4]{8\pi}}{\sqrt{s}}$ .

The energy of the system "kink + bound fermion (antifermion)" may be well approximated by the following simple expression:

$$E_{\pm}(s) = \frac{2}{3} \left( \beta(s) + \frac{1}{\beta(s)} \right) \pm \varepsilon(s). \quad (3.1)$$

The function  $E_+(s)$  is shown in Fig. 3b. Notice that for each  $s \in (1; +\infty)$  the energy of the field configuration  $E_+(s)$  is smaller than the energy of the configuration "undistorted



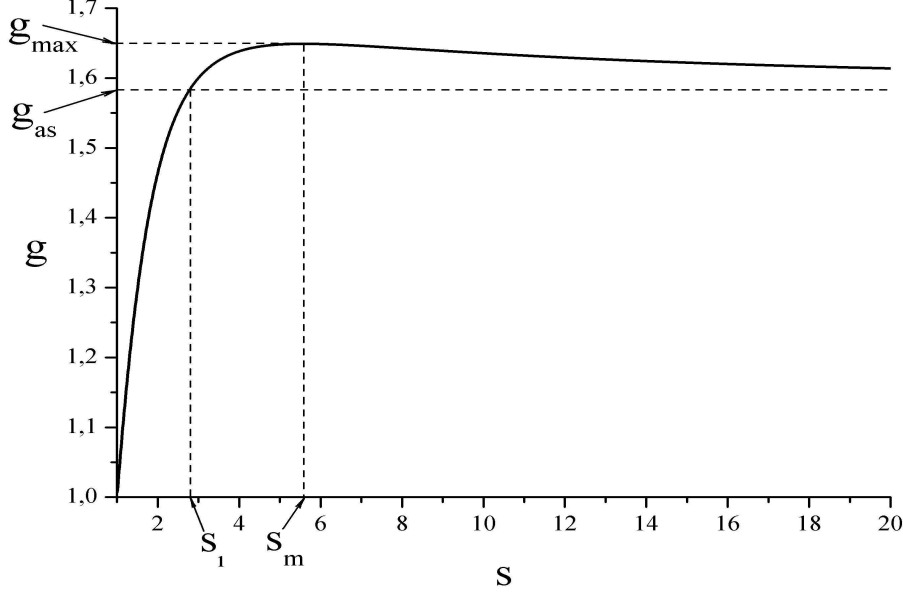


Figure 4: coupling constant  $g$  depending on parameter  $s$ .

domain wall + fermion at rest in continuum". The energy of the latter configuration  $E_{free}(s) = \frac{4}{3} + g(s)$  is also shown in Fig. 3b. Looking at this figure we conclude that the field configuration "kink + excited fermion" is truly bound.

Now let us consider the dependences of observables in terms of coupling constant  $g = g(s) = s \alpha(s)$ . The curve  $g(s)$  is shown in Fig. 4. As it is seen, the function  $g(s)$  reaches its maximum  $g_{max} \approx 1.65$  at  $s_m \approx 5.58$  and falls down for large  $s \gg 1$  reaching  $g_{as} = \sqrt[4]{2\pi} \approx 1.58$  at  $s \rightarrow +\infty$ . The asymptotic behaviour of  $g(s)$  is:

$$g(s) = \sqrt[4]{2\pi} \left( 1 + \frac{3}{8s} \right).$$

The crossing point  $g(s_1) = g_{as}$  is also marked in Fig. 4 with  $s_1 \approx 2.78$ .

The energy of the system  $E_{\pm}(g)$  as a function of coupling constant is shown in Fig. 5. Note that in the interval  $1 \leq g < g_{as}$  ( $1 \leq s < s_1$ ) the functions  $E_+(g)$  and  $E_-(g)$  are single-valued, whereas in the interval  $g_{as} < g \leq g_{max}$  ( $s_1 \leq s < +\infty$ ) they are double-valued. So for each  $g \in (g_{as}; g_{max}]$  there are different branches of the solution for both  $E_+(s)$  and  $E_-(s)$ . The first branch of function  $E_+(s)$  corresponds to the interval

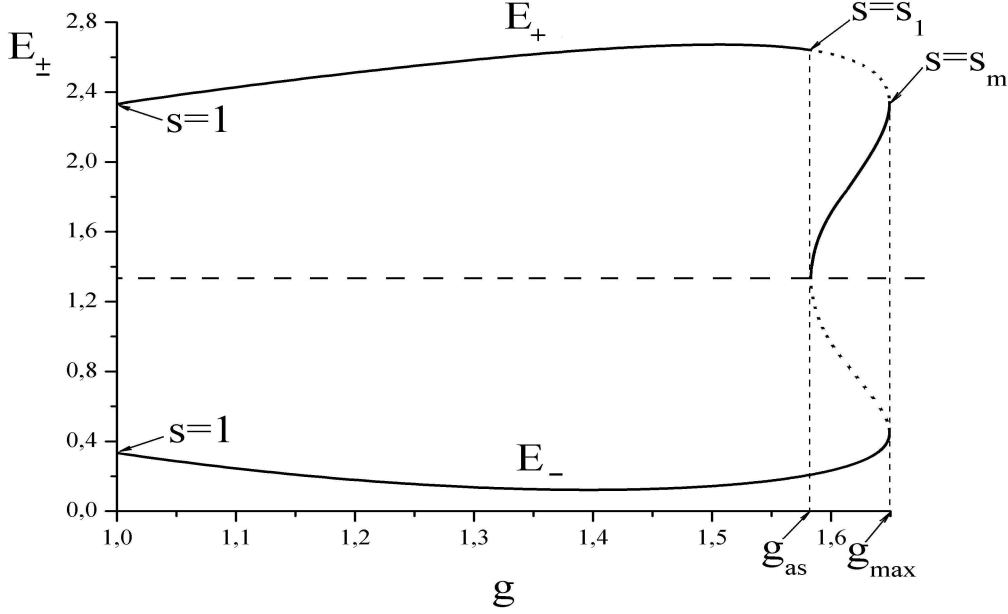


Figure 5: total energy  $E_{\pm}$  of the system as a function of coupling constant  $g$ ; stable branches of the solution are shown by solid lines; unstable branches are indicated by dotted lines. Horizontal dashed line demonstrates the energy of the undistorted kink.

$s \in [s_1; s_m]$ . The second branch corresponds to  $s \in [s_m; +\infty)$ . As it is seen from Fig. 5, the first branch of solution  $E_+(s)$  has larger energy  $E(g(s))$  than the second one. That is why the first branch is unstable with respect to the decay into the second branch. The excess of energy could be emitted in the form of waves of scalar field  $\phi$ . The unstable branch of the solution is drawn in Fig. 5 by dotted line. Analogous situation takes place for function  $E_-(s)$ . Stable branch of solution for function  $E_-(s)$  is also shown in Fig. 5 by solid line.

The lower stable branch for function  $E_+(s)$  corresponds to large  $s \in [s_m; +\infty)$ . As it follows from Fig. 3a, in this region  $\varepsilon(s)$  is small and  $\varepsilon(s) \rightarrow 0$  at  $s \rightarrow +\infty$  (or  $g \rightarrow g_{as}$ ). That is why it is quite natural to call this branch the "quasi zero-mode" solution.

So we got two distinct stable branches for field configurations: domain wall carrying an excited fermion. Let us discuss what these field configurations look like.

The r.h.s. of Eq. (2.5)  $F(x, s)$  is proportional to the product  $u_{\varepsilon'}(x)v_{\varepsilon'}(x)$ . For different

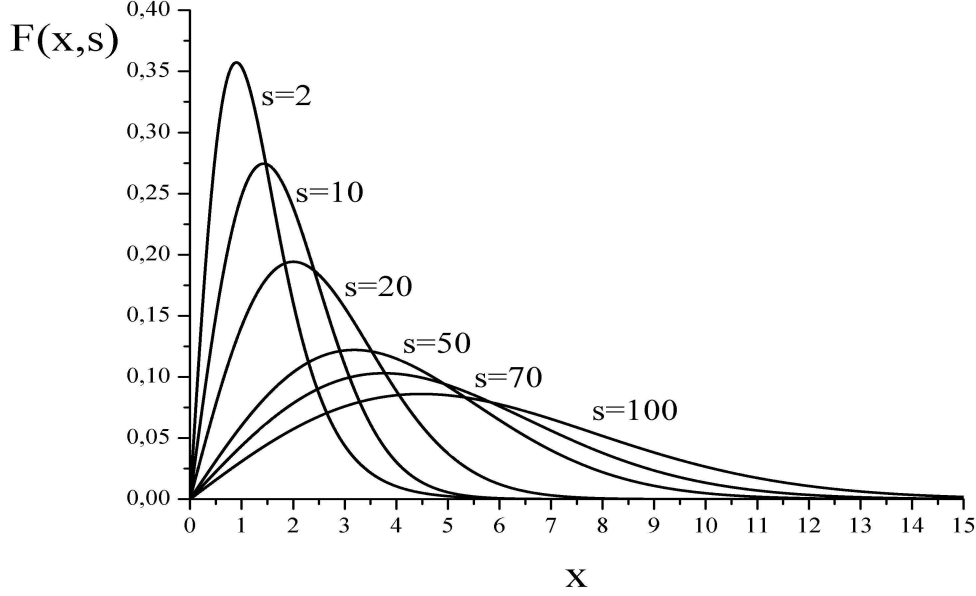


Figure 6: the right-hand side of eq. (2.5) as a function of  $x$  for some values of  $s$ .

values of parameter  $s$  the function  $F(x, s)$  is shown in Fig. 6. The maximum position for each curve is at  $x_{max} = \frac{\sqrt{s}}{\sqrt[4]{8\pi}}$  ( $s \gg 1$ ), and

$$F(x_{max}, s) = \sqrt{\frac{2}{es}}.$$

So in the limit of large  $s$ , i.e. for  $g \rightarrow g_{as} = \sqrt[4]{2\pi}$ , the r.h.s. of Eq. (2.5) becomes small and as a result the profile of the domain wall looks similar to the unperturbed kink  $\phi_K = \tanh x$ .

Let us clarify what the wave function of fermion looks like in the limit of large  $s \gg 1$ . The position of the maximum of  $u_{\varepsilon'}^2(x)$  is at  $\tilde{x}_{max} = \frac{\sqrt{s}}{\sqrt[4]{2\pi}}$  and

$$u_{\varepsilon'}^2(\tilde{x}_{max}) = \sqrt[4]{\frac{2}{\pi e^4}} \frac{1}{\sqrt{s}}.$$

Some profiles of  $u_{\varepsilon'}^2(x)$  are presented in Fig. 7a. We conclude that in the limit of large  $s$  the upper component of the fermionic wave function is located outside the domain wall.

On the contrary, the maximum of the lower component  $v_{\varepsilon'}(x)$  is at  $x = 0$ , i.e. on the

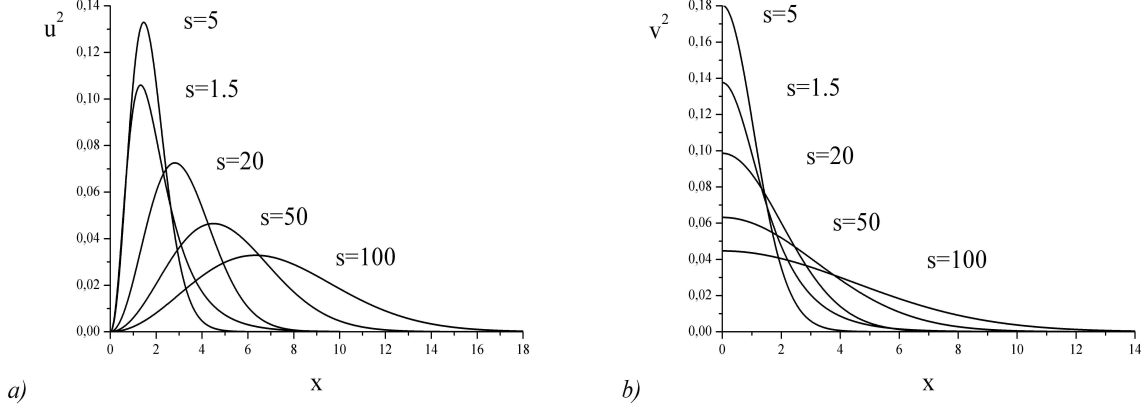


Figure 7: the functions  $u_{\varepsilon'}^2(x)$  (figure a) and  $v_{\varepsilon'}^2(x)$  (figure b) for some values of  $s$ .

domain wall, for all values of  $s \in (1; +\infty)$  and

$$v_{\varepsilon'}^2(0) = \frac{1}{\sqrt[4]{8\pi}} \frac{1}{\sqrt{s}}.$$

In the limit of large  $s$ ,  $v_{\varepsilon'}(x) \sim \exp(-g_{as}|x|)$  ( $|x| \rightarrow +\infty$ ). The function  $v_{\varepsilon'}(x)$  behaves as a zero-mode solution in the limit of large  $s$ . Some profiles of  $v_{\varepsilon'}^2(x)$  are presented in Fig. 7b.

Thus, in the limit of large  $s$  the wave function of a fermion in the first excited state practically splits into two parts. The upper component of the wave function,  $u_{\varepsilon'}(x)$ , which describes fermions with spin projection  $+1/2$ , is located outside the domain wall. The lower component of the wave function,  $v_{\varepsilon'}(x)$ , with spin projection  $-1/2$ , prefers smaller distances from domain wall. As a result, in the limit of large  $s$  the domain wall separates the maxima of the upper  $u_{\varepsilon'}(x)$  and the lower  $v_{\varepsilon'}(x)$  components of the fermionic wave function in space.

## 4 Conclusion

We used a simple variational method and found a solution of the problem "domain wall + excited fermion". We performed numerical simulations. For each coupling constant  $g \in (1; g_{max}]$  the solution is a bound fermion with wave function (2.2) in the field of

the distorted kink  $\tilde{\phi}_K = \tanh(\beta(s)x)$ . The functions  $\alpha(s)$  and  $\beta(s)$  are shown in Fig. 1. Parameter  $s$  varies in the interval  $1 < s < +\infty$ . This corresponds to a variation of coupling constant  $g$  in the limits

$$1 < g \leq g_{max} \approx 1.65.$$

No solution for a fermion in the first excited state on the domain wall was found for any  $g > g_{max}$ .

For  $g \in (1; g_{max}]$  we found two separate stable solution branches for function  $E_+(s)$ . For  $s \in (1; s_1)$ , where  $s_1 = 2.78$  and  $g(s_1) = g_{as} = \sqrt[4]{2\pi} \approx 1.58$ , the fermion wave function is located on the distorted domain wall. For  $s = 2$  ( $g = g_1 = 2\sqrt{2(2 - \sqrt{3})}$ ), belonging to this interval, our variational procedure reproduces the exact self-consistent solution of the problem, obtained in our previous publication [1].

For  $s \in [s_1; s_m]$ , where  $s_m = 5.58$ , the solution is unstable.

For the interval  $s \in [s_m; +\infty)$ , which corresponds to the variation of coupling constant  $g \in [g_{max}; g_{as})$ , the fermionic wave function consists of two different pieces approximately separated in space. The upper component  $u_{\varepsilon'}(x)$  is located outside the domain wall and the lower one  $v_{\varepsilon'}(x)$  prefers smaller distances. Note that  $\int_{-\infty}^{+\infty} |v_{\varepsilon'}(x)|^2 dx = \frac{1}{2}$ , which means that only one half of the fermionic wave function is located near the domain wall in this regime of large  $s$ . The profile of the domain wall for these large  $s$ , almost restores its original profile  $\phi_K = \tanh x$ , as  $\beta(s) \rightarrow 1$  at  $s \rightarrow +\infty$ .

Note that the energy of the fermion,  $\varepsilon(s)$ , is getting very small in the limit of large  $s$  (see also Fig. 3a). We conclude that in this limit,  $s \gg 1$ , the spectrum of the problem "domain wall + fermion" has two nearly degenerate states: the zero-mode ground state ( $\varepsilon = 0$ ) and the state with an excited fermion. The energy of the latter is  $\varepsilon(s) \approx \frac{\sqrt[4]{8\pi}}{\sqrt{s}} \ll 1$ , so this level may be classified as a quasi zero-mode solution. For  $g \geq g_{max}$  only zero-mode solution survives. The picture is slightly different for an antifermion on the domain wall (function  $E_-(s)$ ). For this case the stable branch of solution corresponds to  $s \in (1; s_m)$  ( $g \in (1; g_{max})$ ).

Speaking of the practical applications of the results discussed above, we should first of all mention the problems of cosmology. In this connection we refer to the classical studies of Refs. [11, 12, 13].

Note that a similar problem "kink + charged scalar field" at classical level was solved in Ref. [14]. A related problem of the interaction of a domain wall with a skyrmion was studied in Ref. [15].

Some other properties of fermions in the fields of topological objects such as solitons and instantons one may also find in the monography by R. Rajaraman [16].

## 5 Acknowledgments

The authors are thankful to A. A. Abrikosov, O. V. Kancheli and W. J. Zakrzewski for useful discussions and to V. A. Lensky for his careful reading of the manuscript and for many useful remarks. This work was partially supported by the Russian State Atomic Energy Corporation "Rosatom" and by grant NSh-4172.2010.2.

## References

- [1] *V. A. Gani, V. G. Ksenzov, A. E. Kudryavtsev*, *Yad. Fiz.* **73**, num. 11 (2010); arXiv: 1001.3305 [hep-th].
- [2] *R. Dashen, B. Hasslacher, A. Neveu*, *Phys. Rev.* **D10**, p. 4130 (1974).
- [3] *M. B. Voloshin*, *Yad. Fiz.* **21**, p. 1331 (1975).
- [4] *R. Jackiw, C. Rebbi*, *Phys. Rev.* **D13**, p. 3398 (1976).
- [5] *J. Goldstone, F. Wilczek*, *Phys. Rev. Lett.* **47**, p. 986 (1981).
- [6] *D. Stojkovic*, *Phys. Rev.* **D63**, 025010 (2001); hep-ph/0007343.
- [7] *Yi-Zen Chu, T. Vachaspati*, *Phys. Rev.* **D77**, 025006 (2008); arXiv: 0709.3668 [hep-th].

- [8] *Y. Brihaye, T. Delsate*, Phys. Rev. **D78**, 025014 (2008); arXiv: 0803.1458 [hep-th].
- [9] *T. I. Belova, A. E. Kudryavtsev*, Phys. Usp. **40**: 359-386, 1997; Usp. Fiz. Nauk **167**: 377-406, 1997.
- [10] *V. A. Rubakov*, "Classical Gauge Fields" (in Russian). Editorial URSS, Moscow, 1999.
- [11] *Ya. B. Zel'dovich, I. Yu. Kobzarev, L. B. Okun*, Zh. Eksp. Teor. Fiz. **67**, p. 3 (1974); Sov. Phys. JETP **40**, p. 1 (1975).
- [12] *M. B. Voloshin, I. Yu. Kobzarev, L. B. Okun*, Yad. Fiz. **20**, p. 1229 (1974).
- [13] *V. A. Berezin, V. A. Kuzmin, I. I. Tkachev*, Phys. Lett. **B120**, p. 91 (1983).
- [14] *V. A. Lensky, V. A. Gani, A. E. Kudryavtsev*, Zh. Eksp. Teor. Fiz. **120**, p. 778 (2001); hep-th/0104266.
- [15] *A. E. Kudryavtsev, B. M. A. G. Piette, W. J. Zakrzewski*, Phys. Rev. **D61**, 025016 (2000).
- [16] *R. Rajaraman*, "Solitons and instantons". North-Holland Publishing Company, Amsterdam – New York – Oxford, 1982.